Euro. Jnl of Applied Mathematics (2007), *vol.* 18, *pp.* 571–582. © 2007 Cambridge University Press
doi:10.1017/S0956792507007115 Printed in the United Kingdom

Strain in layered nanocrystals

Y. BAE[1] and R. E. CAFLISCH[2]

[1]*ACMS, University of Arizona, Tucson, AZ, USA*
e-mail: byouri@acms.arizona.edu
[2]*Department of Mathematics, UCLA, Los Angeles, CA, USA*
e-mail: caflisch@math.ucla.edu

(*Received 21 June 2007*)

Layered nanocrystals consist of a core of one material surrounded by a shell of a second material. We present computation of the atomistic strain energy density in a layered nanocrystal, using an idealised model with a simple cubic lattice and harmonic interatomic potentials. These computations show that there is a critical size r_s^* for the shell thickness r_s at which the energy density has a maximum. This critical size is roughly independent of the geometry and material parameters of the system. Interestingly, this critical size agrees with the shell thickness at which the quantum yield has a maximum, as observed in several systems and thus leads one to support the hypothesis that maximal quantum yield is strongly correlated with maximal elastic energy density.

1 Introduction

Layered nanocrystals consist of a core of one material surrounded by a shell of a second material. Synthesis of layered nanocrystals with precise control over their size and shape has been achieved by a number of research groups [1, 4, 5, 6] and provides an effective method for designing material systems with desired optoelectronic properties [4]. In particular, the photostability (hole confinement in the core), electronic accessibility (electron spreading into the shell), and high quantum yield make these core–shell nanocrystals very attractive for use in optoelectronic devices [6].

Because of the small size of these systems, their atomic structure is epitaxial in many cases. Lattice mismatch between the materials in the core and the shell leads to elastic strain in a layered nanocrystal. This strain has both structural and optoelectronic consequences. If the strain is large enough, then it is relieved by irregular growth of the shell [4]; i.e., the epitaxial structure is lost. As a result, the shell may break off from the core [4]. Quantum yield for a layered nanocrystal has been found to correlate with strain [1].

The present study employs a simple model for the structure and strain of a layered nanocrystal. Simulation of this model for a range of geometric and elastic parameters shows that there is a critical shell size at which strain has maximal influence. Moreover, this critical shell size correlates well with the shell size at which quantum yield is maximal.

We shall show that the elastic energy density of a nanocrystal is concentrated near the interface between core–shell and that its maximal value as a function of shell thickness has a peak with small shell thickness. We define this shell thickness as critical shell thickness and compare and contrast these results with the known photoluminescence quantum yield

results from experiments in [6]. Furthermore, we examine the sensitivity of the critical shell thickness to material parameters and the size of core.

The strain model is presented in Section 2, and the computational results of the resulting strain for a nanocrystal are presented in Section 3. Section 4 contains a discussion of the results and their implications. Conclusions and prospects for further work are discussed in Section 5.

2 Atomistic strain model

A typical nanocrystal contains a relatively small number of atoms (i.e. several thousand or less) so that continuum elasticity is not appropriate. We employ a lattice statics model, consisting of atoms whose positions are displaced from a regular grid. Since the goal of this study is qualitative properties of nanocrystals, an idealised model is appropriate. For the geometry, we use a simple cubic lattice, with different equilibrium lattice constants for the core and shell materials. Since all of the cubic systems of Bravais lattice groups have the same symmetry of elastic constants, we expect to obtain qualitative properties of nanoscale systems, using a simple cubic lattice. For the atomistic energy, we use harmonic potentials, which are equivalent to linearized springs between the atoms and bonds. To access the full range of elastic parameters, we allow nearest neighbor springs, diagonal springs, and bond-bending springs, the last of which involves three-body interactions. Further study using nonharmonic potentials is beyond the scope of this work and will be addressed in further study.

The resulting discrete energy density at a discrete point x can be written in the form

$$E = \sum_{k,p} \alpha_k^p \left(S_{kk}^p\right)^2 + \sum_{k \neq l,p,q} \{2\beta_{kl}^{pq} \left(S_{kl}^{pq}\right)^2 + \gamma_{kl}^{pq} S_{kk}^p S_{ll}^q\}, \tag{2.1}$$

where p, q is $+$ or $-$ and k, l is 1, 2 or 3 for a discrete strain component S_{kl}^{pq}. This represents the energy at a discrete point for a 'ball-and-spring' system on a three-dimensional (3D) cubic lattice with variable spring constants, in which k and l denote the three possible lattice vectors, $p = \pm$ signifies the springs in the positive $(+)$ or negative $(-)$ directions along a given lattice vector and (for example) the coefficient α_k^+ is an elastic coefficient related to the spring in the positive kth direction. For consistency between the discrete and continuum energy densities, we can get the elastic coefficients from the Voight constants as

$$(\alpha, \beta, \gamma) = (C_{11}, C_{44}, C_{12})/4. \tag{2.2}$$

The term $S_{kk}^{\pm}$ is a discrete analogue of an elastic strain component; specifically, it is the kth component of the displacement for the spring in the $\pm k$th direction from x. In other words, the bond displacement at the point x is

$$\mathbf{d}^{k\pm} = D_k^{\pm}\mathbf{u} - \varepsilon_k, \tag{2.3}$$

where $D_k^{\pm}$ is the finite difference operator, $\mathbf{u}$ the displacement, and ε_k the relative magnitude of the lattice distortion in the interface, e.g., lattice mismatch. Then, the discrete strain

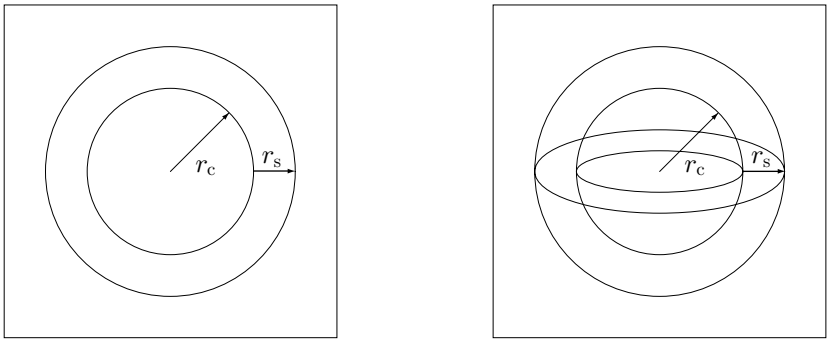

(a) 2D (b) 3D

FIGURE 1. Basic geometry of core–shell nanocrystal model.

components are given by

$$S_{kk}^{\pm} = d_k^{k\pm}, \tag{2.4a}$$

$$S_{kl}^{pq} = \left(d_k^{lq} + d_l^{kp}\right)/2, \tag{2.4b}$$

in which k and l are 1, 2 or 3 (denoting the component number of the bond) and p and q are $+$ or $-$ (denoting positive or negative direction along that component).

The total elastic energy of the system is the sum of the discrete energy densities for each of the atoms. The force balance equations are obtained by setting the variation of the elastic energy with each of the displacements equal to zero.

In core–shell epitaxial growth, strain is induced by mismatch between the lattice constants in the core and those in the shell. Denote the lattice constants in the core and shell as l_c and l_s, respectively. For bonds connecting a core atom and a shell atom, the rest length is taken to be the average $(l_c + l_s)/2$. Similarly, the elastic coefficients for the bonds connecting a core atom and a shell atom are taken to be the averages of the elastic coefficients for the pure materials.

The significant geometric parameters are the core radius r_c, the shell thickness r_s and the lattice mismatch,

$$\epsilon = \frac{l_c - l_s}{l_c}. \tag{2.5}$$

The core consists of atoms whose lattice position x (before displacement) satisfies $|x| \leqslant r_c$, and the shell consists of atoms with $r_c < |x| \leqslant r_c + r_s$, as shown in Figure 1.

3 Critical thickness: Simulation results

Computational results are presented here from minimisation of the total elastic energy (after removing degenerate modes corresponding to translation and rotation), corresponding to balance of all of the forces in the system for 2D (circular, or equivalently rods of infinite length) and 3D (spherical) nanocrystals. For the harmonic potentials used here,

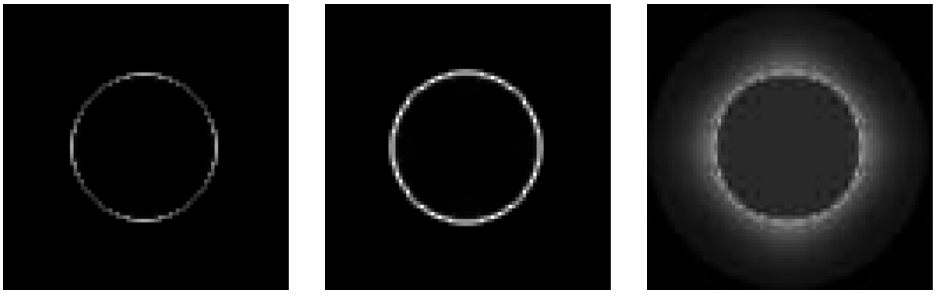

(a) (b) (c)

FIGURE 2. Elastic energy density of 2D layered nanocrystals with core size $r_c = 20$ monolayers and with shell thickness r_s of size (a) 1 monolayer, (b) 2 monolayers and (c) 20 monolayers.

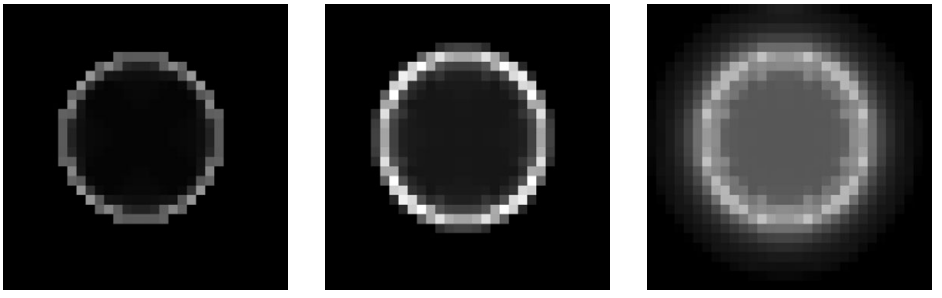

(a) (b) (c)

FIGURE 3. Elastic energy density on an equatorial cross section for 3D layered nanocrystals with core size $r_c = 8$ monolayers and with shell thickness r_s of size (a) 1 monolayer, (b) 2 monolayers and (c) 7 monolayers.

this amounts to solving a linear system of equations, in which the forcing terms come from the lattice mismatch ϵ. The simulation results include values of the displacements, the forces and the energy density. Graphical results will be presented for the last of these. As a figure of merit for the atomistic strain field in a nanocrystal, we shall use the maximum value E_m of the discrete energy density. Since the energy at each atom consists of elastic energy and bond energy, the maximum elastic energy may be a good indicator of strain-driven instability.

3.1 Elastic energy density

Figures 2 and 3 show the elastic energy density of 2D and 3D layered nanocrystals, respectively, of fixed core size r_c for various values of shell thickness r_s. In the 2D nanocrystal simulation (Figure 2), the shell has thickness values $r_s = 1$, 2 and 20 monolayers, on a core of radius $r_c = 20$ monolayers. In the 3D nanocrystal simulation (Figure 3), the shell has thickness values $r_s = 1$, 2 and 7 monolayers, on a core of radius $r_c = 8$ monolayers. For all of these simulations, the elastic constants are $\alpha = 5$, $\beta = 1$ and $\gamma = 3$ and lattice mismatch is $\epsilon = 0.04$.

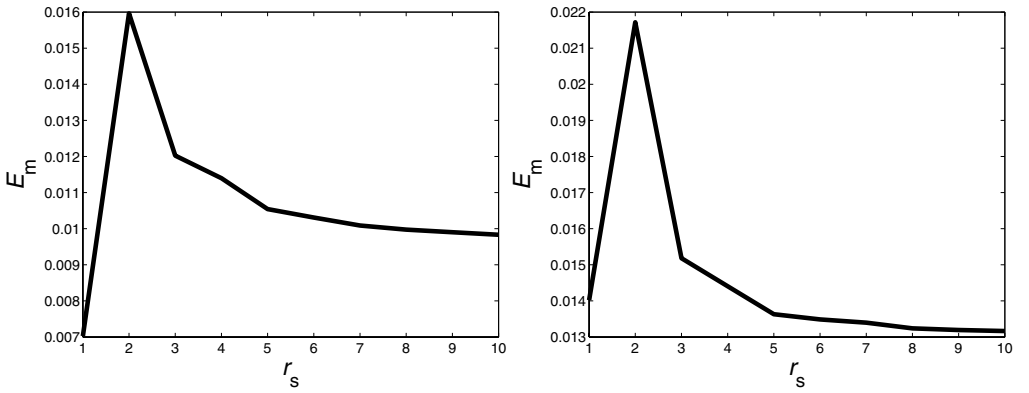

(a) 2D (b) 3D

FIGURE 4. Maximum energy density E_m versus shell thickness r_s for (a) 2D and (b) 3D nanocrystal of core radius $r_c = 8$ monolayers.

We have simulated energy density for a nanocrystal that is larger than the physical system, since the energy distribution is qualitatively similar but more easily seen in the larger system. As the core radius increases, the number of atoms along the interface also increases, so that we can more readily examine the discrete energy density along the interface. In the 3D simulations of Figure 3, the core radius $r_c = 8$ monolayers is a few monolayers larger than the typical physical system. The 2D simulations of Figure 2 use $r_c = 20$ monolayers so that the strain energy distribution exhibits features that are nearly those of a continuum system.

In these figures, the gray scale ranges from black for $E = 0$ to white for $E = E_m$ in which E_m is the largest value of E among the three subfigures; i.e. the scales are the same for the different subfigures. The black region outside of each nanocrystal is a vacuum where there is no energy. Both Figures 2 and 3 show that the energy is concentrated in the region of the shell, along the interface with the core. As the shell thickness increases, the strain energy becomes more concentrated near the shell/core interface, even though the maximum energy density decreases for larger shell thickness. In addition, the largest values of the energy density are close to the diagonal.

3.2 Critical thickness

Figure 4 shows the maximum energy density for a layered nanocrystal, as a function of shell thickness r_s, for fixed values of the other parameters, core size r_c and elastic constants α, β, γ and ϵ. Figure 4 shows that the maximum energy density increases with increasing shell thickness r_s up to a critical shell thickness r_s^*. For $r_s > r_s^*$, the maximum energy density is decreasing as a function of r_s. The general similarity between the critical shell thickness in 2D and 3D is indicative of the robustness of this result. The physical core radius of CdSe/CdS core–shell nanocrystal ranges from 11.5 Å to 19.5 Å, which is equivalent to core radius of 3 monolayers to 6 monolayers, since one full monolayer is approximately 3.5 Å [6].

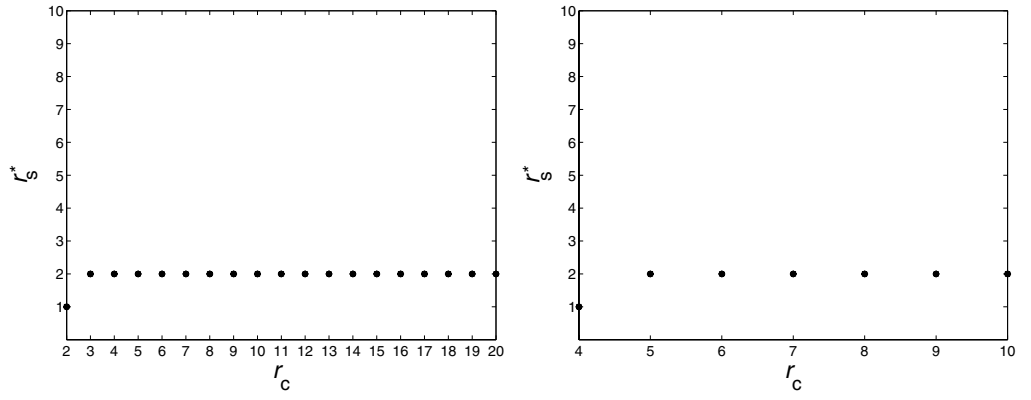

FIGURE 5. Critical thickness r_s^* versus core size r_c for (a) 2D and (b) 3D nanocrystal.

Next we examine the critical shell thickness r_s^* and its dependence on the material and geometric parameters of the nanocrystal, in particular, the dependence of r_s^* on the core size r_c, lattice mismatch ϵ and elastic parameters α, β and γ.

Figure 5 shows weak sensitivity of critical shell thickness r_s^* on the core radius r_c. The critical thickness r_s^* is uniformly 2 monolayers as long as the core size is big enough. We interpret this to be caused by the number of steps along the core–shell interface. Steps along the outer edge of the shell tend to lower strain energy density, but those along the core–shell interface maximise strain effect. For smaller size of core, the number of steps on the core–shell interface is insufficient to increase the strain energy density. For larger core size, the interaction is weak between the core–shell interface and the outer edge of the shell so that the strain energy density is not large. In between there is a critical thickness when the strain energy density is maximal. In simulation, for smaller core size than 3 monolayers for 2D layered nanocrystals and 5 monolayers for 3D layered nanocrystals, the maximum elastic energy density E_m occurs at 1 monolayer of shell thickness r_s.

We have systematically studied the critical shell thickness r_s^* as a function of the elastic parameters α, β and γ and the lattice mismatch ϵ for 2D and 3D nanocrystals. The physically relevant elastic parameters need to satisfy $\alpha > \gamma$ in cubic crystals in order to have positive elastic energy density described in (2.1). We find that the critical shell thickness r_s^* of nanocrystals is independent of elastic parameters as long as the set of elastic parameters α, β and γ satisfies $\alpha > \gamma$. Moreover, we find that the critical shell thickness r_s^* is independent of the lattice misfit ϵ; i.e. the critical shell thickness is the same for all values of lattice misfit ϵ with $\epsilon > 0$.

4 Discussion

4.1 Step interactions

Since the continuum limit of the core–shell nanocrystal corresponds to a shell that is atomistically thick, the critical shell thickness cannot be explained with continuum elasticity. Some insight into the existence of a critical shell thickness r_s^* comes from

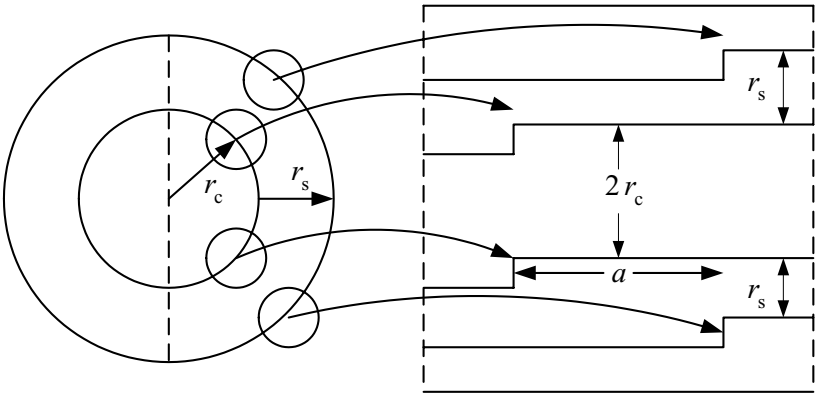

FIGURE 6. Simplified model for step interaction between core and shell, as a thin film system consisting of vacuum, shell layer, core layer, shell layer and vacuum, with a periodic step train on each of the four interfaces.

consideration of step interactions. The strain field produced by a surface step, on an epitaxial surface, interacting with a buried step, on the interface between an epitaxial thin film and the substrate has been successfully studied in [7] using discrete harmonic potentials developed in [2]. We now try to understand step relaxation in core–shell layered nanocrystal system in a way that is analogous to that in [7]. Note that this discussion is based on the use of harmonic potentials and a simple cubic lattice. Although we expect that this provides qualitatively correct results, details would certainly be different for a more realistic system.

On the outer edge of the shell, the shell atoms will relax towards their equilibrium lattice constant, lowering the strain energy density. This relaxation will be greatest along the diagonal, where the atoms have the smallest number of neighbors. Also, the relaxation of the outer edge atoms puts additional stress on the atoms at the core–shell interface. On the other hand, along the core–shell interface, shell atoms near the diagonal have the largest number of core atom neighbors and so they have the largest strain. This maximum is increased by their interaction with the atoms along the diagonal on the outer edge, but that interaction decreases as the shell thickness increases. This indicates a critical thickness.

To qualitatively model this step interaction, we consider a 2D thin film consisting of a core layer between two 'shell' layers, with vacuum both below and above the thin film. In addition, there is a periodic step train on each of the four interfaces, with aligned steps on the two core–shell interfaces and on the shell–vacuum interfaces, as shown in Figure 6. The geometric parameters are the core radius r_c, the shell thickness r_s and the step distance a. Thickness of the core is $2r_c$, which is diameter of the core. We simulate this system using the atomistic strain method described above, using shifted periodic boundary conditions to reduce the computation to that over a single period of the step train.

Figure 7 shows that the maximum elastic energy density peaks at small critical thickness r_s^* and small critical step distance a^*, but is nearly independent of a. The similarity between the simulation results for a nanocrystal and the simplified model provides a means for

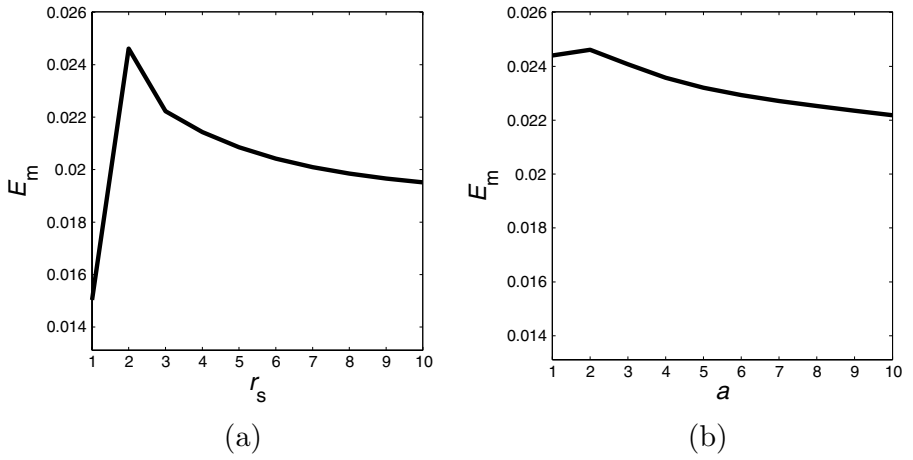

FIGURE 7. The maximum energy density E_m versus (a) shell thickness r_s and (b) step distance a on the core radius $r_c = 5$, for the 2D thin film model pictures in Figure 6, ($\alpha = 5$, $\beta = 1$, $\gamma = 3$ and $\epsilon = 4\%$).

understanding the origin of the critical thickness. We examine the correlation of the shell thickness r_s^* and the step distance a^* for a given core radius r_c. We find that the critical shell thickness r_s^* does not depend on the step separation a and the critical step separation a^* is approximately half the shell thickness r_s. It provides some understanding of the fact that shell atoms near the diagonal have the maximum elastic energy density. This interpretation is also consistent with the independence of the critical shell thickness on the material and geometric parameters of nanocrystals, as shown in Section 3.

4.2 Comparison to quantum yield

The critical shell thickness, observed in the simulations presented above, correlates closely to the maximum value of the quantum yield from experiments. Since high photoluminescence quantum yield is crucial in fabrication of optoelectronic device, the photoluminescence quantum yield (QY) has been an indicator of high quality of devices. Photoluminescence quantum yield data presented below come from both CdSe/CdS [6] and InAs/CdSe [1] layered nanocrystals.

Figure 8 shows a comparison between the quantum yield QY and maximum energy density E_m as a function of shell thickness r_s. The dotted line represents the strain simulation results, and the solid line represents the quantum yield results. The core radii of the CdSe/CdS nanocrystals are $19.5\,\mathring{A}$ and $110\,\mathring{A} \times 20\,\mathring{A}$, respectively, which are approximately 5.5 and 5.7 monolayers, respectively, since each monolayer is approximately $3.5\,\mathring{A}$. The core radius used in the strain simulation is $r_c = 5$ monolayers. To compare the qualitative behaviour of QY and E_m, we scaled the strain simulation results to have the same maximum as that of the quantum yield. Both quantum yields results have the peak at the small shell thickness. Strain has been cited as a probable cause of high quantum yield in [1, 5].

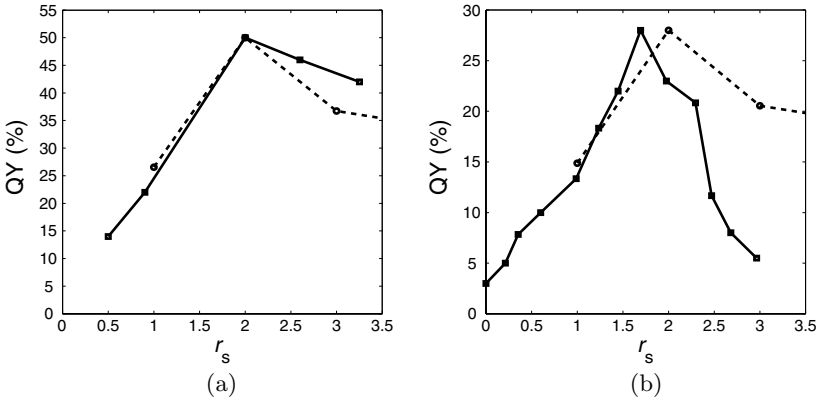

FIGURE 8. Comparison of quantum yield QY (–) and E_m (- -) as a function of shell thickness r_s for core radius $r_c = 5$ monolayers. E_m has been scaled so that its maximum value is the same as that of QY. The experimental measurements of QY are for (a) photoluminescence quantum yield of CdSe/CdS core–shell nanocrystal with shell thickness on core radius of 19.5 $\mathring{A}$ [6], (b) fluorescence quantum yield of CdSe/CdS core–shell nanorod with shell thickness on core radii of 110 $\mathring{A} \times 20\,\mathring{A}$ [5].

4.3 Continuum limit of nanocrystals

As a check on the atomistic computations, we solve the analogous equations for continuum elasticity. Our atomistic strain model is consistent with finite difference equations of continuum elasticity, so we expect that atomistic strain computation is consistent with continuum elasticity. The continuum limit is a nanocrystal with a large core radius and a thick shell. Therefore, the continuum limit does not have critical thickness in which $E_m(r_s)$ peaks. From the study of continuum limit, we expect to check the atomistic phenomenon and their validation.

We assume that the elastic coefficients are chosen to give isotropic elasticity so that the continuum nanocrystals are isotropic and invariant under rotations with respect to their centres. Therefore, the displacement vector $\vec{u}$ at the position x is a radial function. The equilibrium equation for continuum elasticity is

$$3\beta\Delta\vec{u} + (\alpha + \beta + 2\gamma)\vec{\nabla}(\vec{\nabla}\cdot\vec{u}) = 0 \tag{4.1}$$

and the radial function satisfies $\vec{\nabla} \times (\vec{\nabla} \times \vec{u}) = 0$. With some algebraic computations, we have the resulting equilibrium,

$$\vec{\nabla}(\vec{\nabla}\cdot\vec{u}) = 0. \tag{4.2}$$

The lattice misfit is modeled as producing a pressure that is $-\epsilon$ on the interface between core and shell and 0 on the outer edge of the shell. We recalculate the solution of the continuum elastic equations given in [3]. The elastic energy density in the core is a constant function and density in the shell is bigger than the density in the core. The maximum elastic energy density for both a 2D and a 3D layered nanocrystal occurs along the core–shell boundary. In this paper, we will compare the 2D simulations to the continuum

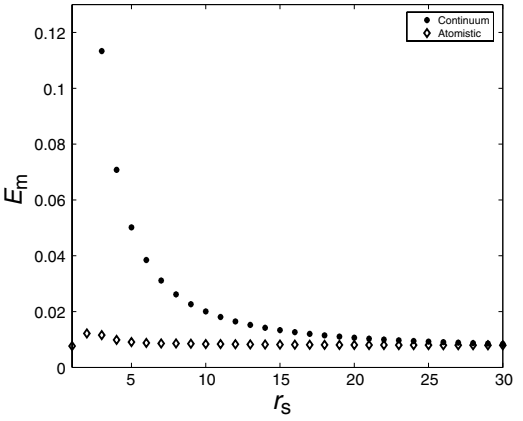

FIGURE 9. The maximum energy density $E_m(r_s)$ from continuum (•) and atomistic (◇) simulations, where r_s ranges from 1 monolayer to 30 monolayers for fixed core radius r_c of 20 monolayers.

solution. From continuum elasticity, the maximum elastic energy density for a 2D layered nanocrystal is given by [3]

$$E_m(r_c, r_s) = \frac{\epsilon^2}{8} \frac{r_c^4}{\left((r_c + r_s)^2 - r_c^2\right)^2} \left\{ \frac{3}{\alpha + \beta + 2\gamma} + \frac{1}{\beta} \frac{(r_c + r_s)^4}{r_c^4} \right\}. \tag{4.3}$$

In Section 3, we have examined the maximum energy density as a function of shell thickness. To compare the continuum limit for a layered nanocrystal, we consider continuum limit with large radius of core and thick shell. Figure 9 shows the maximum energy density E_m as a function of shell thickness r_s for a fixed core radius r_c of 20 monolayers and r_s ranges from 1 monolayer to 30 monolayers. The dots represent the maximum elastic energy density obtained from a continuum elasticity, and the diamonds represent one from an atomistic simulation described in Section 2 for a 2D nanocrystal. Since our simulation calculates energy density as energy per unit lattice cell, we adjust the energy scale by multiplying continuum limit E_m by cell area for a 2D layered nanocrystal or cell volume in three dimensions.

We find E_m from an atomistic simulation converges to one from a continuum elasticity as shell thickness increases. However, the continuum limit does not show any peak for very thin shell in contrast to atomistic simulations. This proves that the critical thickness is atomistic phenomenon that is not present in the continuum theory. The convergence for thicker shell shows that our strain model described in Section 2 is valid for simulating the strain field of a layered nanocrystal.

4.4 Nanorod

A number of research groups have demonstrated a peak of photoluminescence quantum yield for a layered nanorod [1, 4, 5]. Although our model can be applicable to a nanorod of any shape, we will simulate it for the special case of an ellipsoidal spheroid. For a 3D layered nanorod, the geometric parameters are the core radius r_d along the diameter and r_l along the length of rod, and the shell thickness r_s. The core consistsof atoms whose

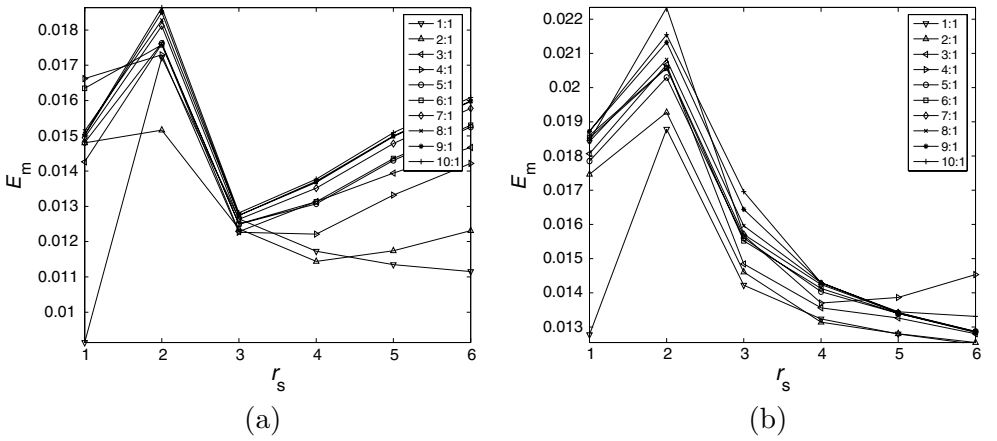

FIGURE 10. A series of plots of $E_m(r_s)$ for aspect ratio $r_l : r_d$ ranging from 2:1 to 10:1 for r_d equal to (a) 5 monolayers and (b) 7 monolayers.

lattice position (x, y, z) satisfies

$$\frac{x^2}{r_l^2} + \frac{y^2 + z^2}{r_d^2} \leqslant 1 \tag{4.4}$$

and shell consists of atoms satisfying

$$\frac{x^2}{r_l^2} + \frac{y^2 + z^2}{r_d^2} > 1 \quad \text{and} \quad \frac{x^2}{(r_l + r_s)^2} + \frac{y^2 + z^2}{(r_d + r_s)^2} \leqslant 1. \tag{4.5}$$

Research on colloidal semiconductor nanocrystals suggested the possibility for the epitaxial strain, depending on the shape of the core varying from nearly spherical to nearly cylindrical. We expect that a series of $E_m(r_s)$ on an aspect ratio $r_l : r_d$ provides one of opportunities to study the strain at the interface.

Figure 10 presents a series of the maximum elastic energy density $E_m(r_s)$ of 3D nanorod for $r_l : r_d$ varying from 1:1 to 10:1 for the core radius r_d equal to 5 monolayers (Figure 10(a)) and 7 monolayers (Figure 10(b)). Both Figure 10(a) and (b) show that the series of E_m curves all peak at the critical thickness r_s^* of 2 monolayers. These results show that the critical shell thickness r_s^* is generally applicable to layered nanorods and nanocrystals.

An increase in E_m was observed in thinner rods for $r_s > r_s^*$. We believe that this effect is a result of the reflection of the strain field, but we have not analysed it yet. Thinner rods have more reflection effect from the relaxation on the outer edge of the shell and strain on the interface of core–shell. The increase in E_m becomes less as the core radius r_d along the diameter increases. This supports the explanation of strain reflection effects.

The research of [4] demonstrated that the planes extending along the diameter of the rod are more compressed than planes extending along the length of the rod. From the fact that the compression along the plane is the trace of the strain tensor, we verified that $S_{xx} + S_{yy} < S_{yy} + S_{zz}$ at every atom, which is consistent with the experimental results. It also implies that the irregular growth occurs along the planes along the diameter, as shown in [4].

5 Conclusion

We have examined the elastic energy density of a nanocrystal and the corresponding critical shell thickness. The simulation results presented above are for a highly idealised model of a layered nanocrystal. The robustness of these results with respect to variation of dimension, geometry and material parameters suggests that these results are qualitative and generally applicable. In addition, there is some evidence that the critical shell thickness found in these simulations is related to the maximal values of quantum yield, as found experimentally.

We have demonstrated the nature of the critical shell thickness by the step–step interaction analysis. A continuum approach also shows that the effect of step interaction is essentially atomistic. The spheroid model generalizes the effect of epitaxial strain at the interface of core–shell nanocrystal. These may lead to determination of the location where thick shell nanorod changes morphologically and grows irregularly.

We expect our atomistic strain computations to provide evidence of the strain effect in nanotechnology. The relation between strain and quantum yield can help to explain why the maximum quantum yield occurs at the thin shell thickness and further shell growth reduces the quantum yield. This suggests that engineering of strain effect may be a fruitful approach to obtaining desired optoelectronic properties in nanoscale devices.

Acknowledgements

The authors thank the Focus Center Research Program of the Semiconductor Research Corporation and its Focus Center on Functional Engineered NanoArchitectonics for the financial and programme support.

References

[1] Cao, Y. W. & Banin, B. (1999) Synthesis and characterization of InAs/InP and InAs/CdSe core–shell nanocrystals. *Angew. Chem. Int. Ed.* **38**, 3692–3694.

[2] Connell, C. R., Caflisch, R. E., Luo, E. & Simms, G. (2006) The elastic field of a surface step: The Marchenko–Parshin formula in the linear case. *J. Comp. Appl. Math.* **196**, 368–386.

[3] Landau, L. D. & Lifschitz, E. M. (1959) *Theory of Elasticity*, Addison-Wesley.

[4] Manna, L., Schoer, E. C., Li, L. S. & Alivisatos, A. P. (2002) Epitaxial growth and photochemical annealing of graded CdS/ZnS shells on colloidal CdSe nanorods. *J. Am. Chem. Soc.* **124**, 7136–7145.

[5] Mokari, T. & Banin, U. (2003) Synthesis and properties of CdSe/ZnS core–shell nanorods. *Chem. Mater.* **15** (20), 3955–3960.

[6] Peng, X., Schlamp, M. C., Kadavanich, A. V. & Alivisatos, A. P. (1997) Epitaxial growth of highly luminescent CdSe/CdS core–shell nanocrystals with photostability and electronic accessibility. *J. Am. Chem. Soc.* **119**, 7019–7029.

[7] Schindler, A. C., Gyure, M. F., Simms, G. D., Vvedensky, D. D., Caflisch, R. E., Connell, C. & Luo, E. (2003) Theory of strain relaxation in heteroepitaxial systems. *Phy. Rev. B.* **67**, 075316.